SERS detection of biomolecules using lithographed nanoparticles towards a reproducible SERS biosensor

2010 Nanotechnology 21 475501

(http://iopscience.iop.org/0957-4484/21/47/475501)

Nanotechnology **21** (2010) 475501 (6pp) doi:10.1088/0957-4484/21/47/475501

SERS detection of biomolecules using lithographed nanoparticles towards a reproducible SERS biosensor

Catalina David[1], **Nicolas Guillot**[1], **Hong Shen**[2], **Timothée Toury**[2] **and Marc Lamy de la Chapelle**[1,3]

[1] Laboratoire CSPBAT (FRE 3043), UFR SMBH, Université Paris XIII, 74 rue Marcel Cachin, F-93017 Bobigny, France
[2] ICD-LNIO-UMR, CNRS 6279, Université de technologie de Troyes, 12 rue Marie Curie, F-10010 Troyes, France

E-mail: marc.lamydelachapelle@univ-paris13.fr

Received 18 August 2010, in final form 23 September 2010
Published 29 October 2010
Online at stacks.iop.org/Nano/21/475501

Abstract

In this paper we highlight the accurate spectral detection of bovine serum albumin and ribonuclease-A using a surface-enhanced Raman scattering (SERS) substrate based on gold nanocylinders obtained by electron-beam lithography (EBL). The nanocylinders have diameters from 100 to 180 nm with a gap of 200 nm. We demonstrate that optimizing the size and the shape of the lithographed gold nanocylinders, we can obtain SERS spectra of proteins at low concentration. This SERS study enabled us to estimate high enhancement factors (10^5 for BSA and 10^7 for RNase-A) of important bands in the protein Raman spectrum measured for 1 mM concentration. We demonstrate that, to reach the highest enhancement, it is necessary to optimize the SERS signal and that the main parameter of optimization is the LSPR position. The LSPR have to be suitably located between the laser excitation wavelength, which is 632.8 nm, and the position of the considered Raman band. Our study underlines the efficiency of gold nanocylinder arrays in the spectral detection of proteins.

1. Introduction

Surface-enhanced Raman scattering (SERS) is a powerful technique for chemical and biological sensing applications. Widely used for ultrasensitive chemical analysis down to single-molecule detection [1–6] its field of application has been expanded from chemical–biochemical analysis to nanostructure characterization and biomedical applications [7–12].

Based on the excitation of localized surface plasmons (LSP), SERS has become a very effective tool to analyse molecules, by greatly increasing the Raman signals coming from molecules which have been adsorbed on metal nanosized structures, in particular Au, Ag or Cu [13–19].

Currently most researchers agree on the existence of two processes in the SERS effect: firstly, the enhancement of the local electromagnetic field [20, 21] and, secondly, the chemical enhancement [22]. The latter enhancement involves the interaction between electronic states of the adsorbed molecule and the surface of the metal. This makes possible a charge transfer between the surface and the adsorbed molecule. This transfer may increase significantly the polarizability of the molecule through the interactions between the electronic states and the metal electrons. However, the dominant contribution to the SERS enhancement is due to the electromagnetic effect (10^{12} enhancement factor), while the chemical effect contributes to the enhancement only by two orders of magnitude. Indeed, when a metallic nanoparticle is irradiated at the resonance frequency of the LSP, its excitation causes a huge enhancement of the local electromagnetic field in the metal particle vicinity and induces an enhancement of the Raman signal of the adsorbed molecules [20, 21].

Extensive studies have revealed that the SERS intensity strongly depends on the localized surface plasmon resonance (LSPR) [20, 23–28]. Different papers dedicated to the study of the influence of the LSPR position on SERS intensity demonstrated that, for cylindrical particles, the maximum

[3] Author to whom any correspondence should be addressed.

enhancement must be obtained for an LSPR wavelength located between the laser excitation wavelength and that of the studied Raman mode [24, 26, 29]. However, the enhancement of the observed signal depends on many parameters, including the nature of the metal, the molecule, the type of roughness and the chemical environment.

The SERS effect can be obtained using different metallic substrates such as metal island films [2, 30–34], aggregated metal colloids [35, 36], electrochemically roughened electrodes [23] or gold and silver colloidal monolayers [37]. In spite of this, due to their complex and irregular structure these substrates often do not lead to uniform, highly sensitive and reproducible SERS effects.

Recent developments in nanofabrication techniques have opened ways to overcome this limitation: nanosphere lithography (NSL) [15] and electron-beam lithography (EBL) [24] permit the manufacture of reproducible nanostructured surfaces with complex patterns. They provide an exceptional opportunity to engineer controllable SERS substrates.

These techniques enable the fabrication of highly reproducible patterns containing nanoparticle arrays with different geometries, shapes and sizes [38–40]. These parameters can be easily modified, thus leading to a spectral shift of the LSPR throughout the visible [26, 40] and IR [41] ranges. In these conditions, the position of the plasmon resonance can be controlled [42]. With such substrates, the SERS enhancement is important ($\sim 10^5$) and strongly depends on the nanoparticle coverage and the position of the studied mode with respect to the wavelength of the plasmon resonance [43].

The present paper is dedicated to a systematic study of SERS efficiency at 632.8 nm excitation wavelength of gold nanocylinder arrays obtained by EBL and having different diameters in order to develop a highly reproducible nanobiosensor. Taking into consideration the lack of SERS studies using these kinds of metallic gratings in the case of biomolecules, the main purpose of our study is to determine the influence of the position of the LSPR on the SERS intensity of proteins.

Since SERS provides important molecular structural information, we carried out SERS spectra of bovine serum albumin (BSA) and bovine pancreatic ribonuclease-A (RNase-A) in order to detect conformational changes and structural differences regarding preferred orientations of the molecules with respect to the metal surface [13, 43].

2. Materials and methods

The gold nanocylinder arrays are fabricated on glass substrates by EBL and lift-off techniques (for more details see [40]). The diameters of the nanocylinders range from 100 to 180 nm while their heights are kept constant at 50 nm, the grating constant between particles being 200 nm (edge to edge). The proteins, BSA and RNase-A, were purchased from Sigma-Aldrich and were used without further purification. All the proteins were prepared at 1 mM concentration in high purity water. The pH of the aqueous solutions at 22 °C was 7.0 for BSA and 8.6 for RNase-A. A drop of each protein was deposited on the SERS substrate until completely dried. The extinction and SERS spectra were recorded with a Jobin-Yvon micro-Raman spectrophotometer (Labram 300). The extinction spectra were recorded in transmission configuration with a 10× objective (NA = 0.25) by removing the edge filters and on an area of $150 \times 150\ \mu m^2$ selected by the confocal hole. The sample was illuminated in normal incidence with collimated white light. The SERS spectra were measured using a 100× magnification objective (NA = 0.90) in back-scattering geometry, with a spectral resolution of 3 cm^{-1} and a spatial resolution about 1 μm. For classical Raman measurements in solution, a macro-objective with a focal length of 40 mm was used (NA = 0.18). All Raman measurements were carried out with the 632.8 nm line of an He–Ne laser. The position of the band maxima was reproducible within ± 1 cm^{-1}. The laser equivalent power density was 1350 Wm^{-2} for SERS measurements.

3. Results and discussion

3.1. SERS measurements

Our SERS measurements were performed for both proteins, BSA and RNase-A. Albumins are the most abundant proteins in blood plasma and they act as transport proteins for numerous endogenous and exogenous compounds [44]. BSA is an albumin with a 66.4 kDa molecular weight and its structure is composed of 583 amino acids. The secondary structure of this protein is, for the most part, helical (70%) [45].

The structure of RNase-A, which plays an important role in the hydrolysis of RNA, is more stable than that of BSA. It contains 124 amino acids (13.7 kDa) whose spatial arrangement describes two types of secondary structure: α-helix and β-sheet.

The vibrational spectrum of BSA was revealed by both classical Raman [46, 47] and SERS spectroscopy [19, 48] a long time ago by different research teams. The spectral assignment of this protein is well known, as well for RNase-A which has been studied extensively by Raman [49, 50] and SERS spectroscopy [19].

In figure 1, we present the SERS spectra measured for BSA and RNase-A at 1 mM in aqueous solution concentration using the lithographed gold nanocylinders as the SERS substrate.

If comparing the SERS spectrum of BSA (figure 1(A(a.))) with the classical Raman spectrum of BSA in powder state (figure 1(A(c.))) or in aqueous solution at 1 mM concentration (figure 1(A(b.))), one can note that the protein adsorption directly on the nanocylinder arrays does not seem to induce important conformational changes in its structure. In the SERS spectrum, we can easily identify the amide I band (1658 cm^{-1}), the protein side chain deformation (1453 cm^{-1}) or even the contribution of the disordered α-helix structure of the BSA in the amide III band (1252 cm^{-1}).

On the other hand, the deposition of one drop of RNase-A in aqueous solution at 1 mM concentration on the gold nanocylinder arrays leads to strong conformational changes of the protein structure. This behaviour is observed when we compare the SERS spectrum (figure 1(B(a))) with the classical

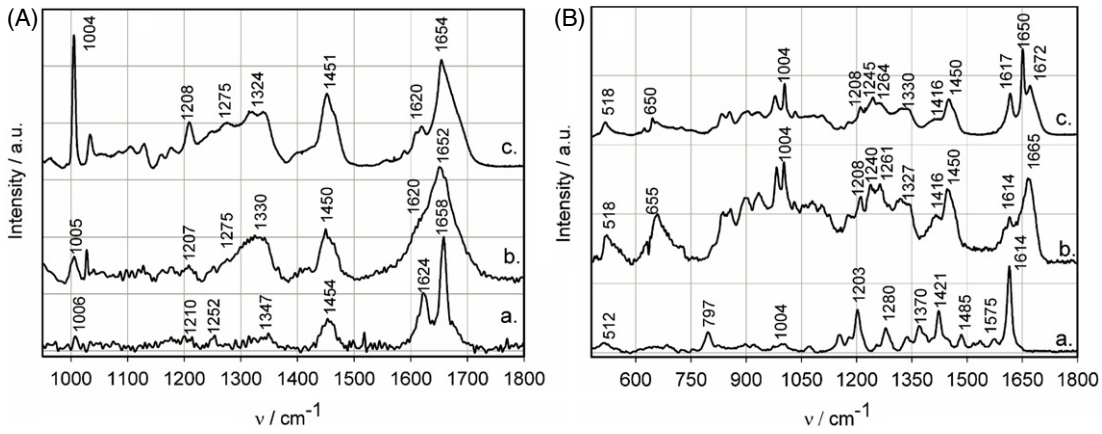

Figure 1. (A) SERS spectrum measured for BSA at 1 mM concentration (a) with acquisition time of 100 s: comparison with the Raman spectra of BSA in aqueous solution at 1 mM (b) and in powder state (c). The intensities were normalized with respect to the intensity of the band located at 1658 cm^{-1}. (B) SERS spectrum measured for RNase-A at 1 mM concentration (a) with acquisition time of 20 s: comparison with the Raman spectra of RNase-A in aqueous solution at 1 mM (b) and in powder state (c). The intensities were normalized with respect to the intensity of the highest band located between 1600 and 1700 cm^{-1}.

Raman spectra in the powder state (figure 1(B(c))) or aqueous solution of the RNase-A (figure 1(B(b))). The lack of the amide band (around 1665 cm^{-1}) in the SERS spectrum strongly indicates that there is a significant change in the secondary structure of RNase-A.

It has been shown that the vibrational bands of the aromatic amino acids are sensitive to the microenvironment upon the protein folding/unfolding process [51–53]. Obviously, the conformational change of RNase-A is highlighted by the presence in the SERS spectrum of strong enhanced vibrational bands specific to the different aromatic amino acid vibrations (Trp and Phe bands located at 1614, 1370, 1203 and 797 cm^{-1}).

From another point of view, if we look closely at the SERS spectra, we can observe that the enhancement of the Raman signal varies as a function of the diameters of the nanoparticles. For a detailed analysis, we represented the SERS intensity of one specific Raman band for each protein as a function of nanocylinder diameters (figures 2(a) and (b)). The considered Raman bands for BSA are the amide I band located at 1658 and 1624 cm^{-1} and for RNase-A the considered Raman band is that located at 1614 cm^{-1} assigned to Trp and Phe ring vibrations. The SERS intensity is estimated from the fit of the Raman bands using a Lorentz function.

Figure 2 shows that the maximum SERS intensity for BSA (figure 2(a)) is obtained in the case of the nanocylinder having a diameter of about 170 nm while for RNase-A (figure 2(b)) this diameter is about 100 nm.

3.2. Estimation of the enhancement factor

We have estimated the enhancement factor of the Raman signal of the amide I band of BSA (1658 cm^{-1}). For this, we have determined the number of molecules excited by the laser beam in the case of two types of measures of BSA at 1 mM concentration: classical Raman in aqueous solution and SERS on gold nanocylinders. The enhancement factor per molecule is defined as [24]

$$G = \left(\frac{N_2}{N_1}\right)\left(\frac{I_{\mathrm{SERS}}}{I_{\mathrm{ref}}}\right). \quad (1)$$

Here N_2 represents the number of molecules excited within the volume of the laser waist for the BSA solution at 1 mM and N_1 is the number of molecules contained in the monolayer deposited on a gold substrate illuminated by the laser spot. The term I_{SERS} is the intensity of the BSA Raman amide I bands recorded on the gold nanoparticles while I_{ref} is the intensity of the same bands in the BSA spectrum measured in aqueous solution at a concentration of 1 mM.

In the case of gold nanocylinders having a diameter of around 170 nm the collection area is about 1.5×10^{-10} m^2 for a pattern that contains 665.6 nanocylinders. Taking into account the fact that the surface of one BSA molecule is about 40×10^{-18} m^2 and assuming that there is a single monolayer of absorbed molecules, N_1 is found to be approximately 3.75×10^5 molecules on the nanocylinder array.

N_2 was estimated from the volume of the laser waist which is approximated to a cylinder with a radius of 150 μm and a depth in the sample of 10 mm. The calculated volume is about 7×10^{-10} m^3 (7×10^{-7} l), thus leading to an N_2 value of approximately 4×10^{12} molecules. According to formula (1), the enhancement factor for the BSA Raman band located at 1658 cm^{-1} is found to be about 10^6.

In the case of RNase-A, we have also estimated an enhancement factor for the vibrational band located at 1614 cm^{-1} in the SERS spectrum. Following the same approach as previously, we found that the collection area is about 8×10^{-12} m^2 and contains 1012.5 nanocylinders with a diameter of 100 nm each. Taking into account that the surface of one RNase-A molecule is 6.0×10^{-18} m^2, the number of RNase-A molecules (N_1) covering the collection area is about 1.33×10^6.

Replacing the data in equation (1), one can obtain the estimated enhancement factor for the band located at

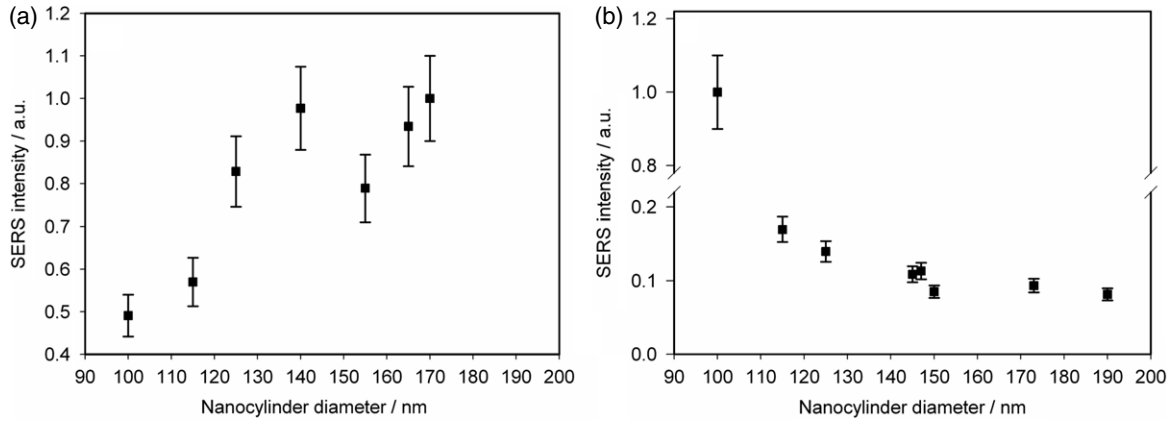

Figure 2. SERS intensity as a function of the nanocylinder diameters: (a) for the BSA Raman bands located at 1614 and 1658 cm^{-1} and (b) for the RNase-A Raman band located at 1614 cm^{-1}. In order to make the error bars more readable in (b) we applied a break on the *Y* axis (between 0.22 and 0.78).

1614 cm^{-1} in the SERS spectra of RNase-A, which is about 10^7.

The estimated values for the enhancement factor are in agreement with those proposed in the literature [24] and show the efficiency of gold nanocylinders in the case of proteins.

Comparing the SERS spectra of the two proteins with their Raman spectra in aqueous solution (as shown in figure 1), we noted that the degradation of the secondary structure of the protein when reacting with the metal surface could give rise to strong Raman enhancement of some aromatic acids from the protein structure. This fact underlines that the Raman cross sections of the studied modes of these proteins remain the same and the SERS effect occurs rather from the enhancement of the local electromagnetic field. Nevertheless, the conformational changes of the protein when deposited on the metallic surface may be overcome by employing the functionalization of the surface, e.g. using antibodies or other intermediate molecules.

3.3. SERS optimization: LSPR characterization

When varying shape, size and distance between the nanoparticles, LSPR positions are shifted to a large extent over the visible spectrum [24, 29]. Therefore we investigated the relation between the position of the LSPR and the Raman enhancement in order to optimize the SERS signal and to use the substrate as a biosensor chip.

In order to find the exact LSPR wavelength to maximize the SERS intensity, we first measured the extinction spectra for each nanocylinder array. At first sight, these spectra (figures 3(a) and (b)) strongly suggest that the protein deposition on the nanocylinders leads to a redshift of the LSPR if compared to the position of the plasmon resonance measured in the presence of air.

The redshift of the LSPR for RNase-A is about 68 nm (figure 3(b)) whereas that in the case of BSA is almost zero with respect to air (figure 3(a)). BSA is a larger protein than RNase-A. We should then assume that the deposition of BSA at the nanocylinder surface leads to a larger change in the dielectric constant of the surrounding medium and thus should lead to a larger redshift of the LSPR. Since it does not correspond to our observation, we suggest that the dipolar mode is shifted in the near-infrared spectral range and that the observed LSPR corresponds to the third order of resonance. This is confirmed by the observation of an increase in the extinction intensity for a wavelength higher than 800 nm. We assume that this increase corresponds to the high frequency side of the dipolar LSPR. In this latter case, the dipolar LSPR should be located close to 950 nm, corresponding to a shift around 250 nm. Since the third order of resonance of nanocylinders gives lower enhancement than the dipolar one [28], this observation can also explain the lower enhancement factor measured for BSA compared to RNase-A.

However, to go further in our analysis, we plotted the SERS intensity as a function of LSPR position for both proteins, as shown in figures 3(c) and (d). Whatever the protein is, one can observe that the maximum enhancement is obtained for an LSPR wavelength located between the laser excitation wavelength and that of the studied Raman mode (that of 1658 cm^{-1} for BSA and of 1614 cm^{-1} for RNase-A). However, due to the LSPR shift towards the third order of resonance, there is no real maximum enhancement in the case of BSA. These results provide evidence that the optimization of the gold nanocylinders' size is required in order to obtain a high enhancement factor and a better sensitivity. Indeed, our study is encouraging but it is obvious that it is necessary to continue with further experiments to improve at the same time the enhancement of the Raman signals of proteins and the detection limit. We saw that the SERS efficiency of these substrates is different from one protein to another and the SERS experience from biomolecules should take into account this consideration. It is not obvious that increasing the nanocylinder diameter will lead to a better enhancement of the Raman signals. In contrast, the position of resonance of the plasmon plays a very important role in the SERS activity. Indeed, as shown in figure 3, the optimization should not be done on the geometrical parameters of the nanocylinders but on their optical properties since in both cases we get the best SERS signal for an LSPR position located between the excitation wavelength and the Raman mode.

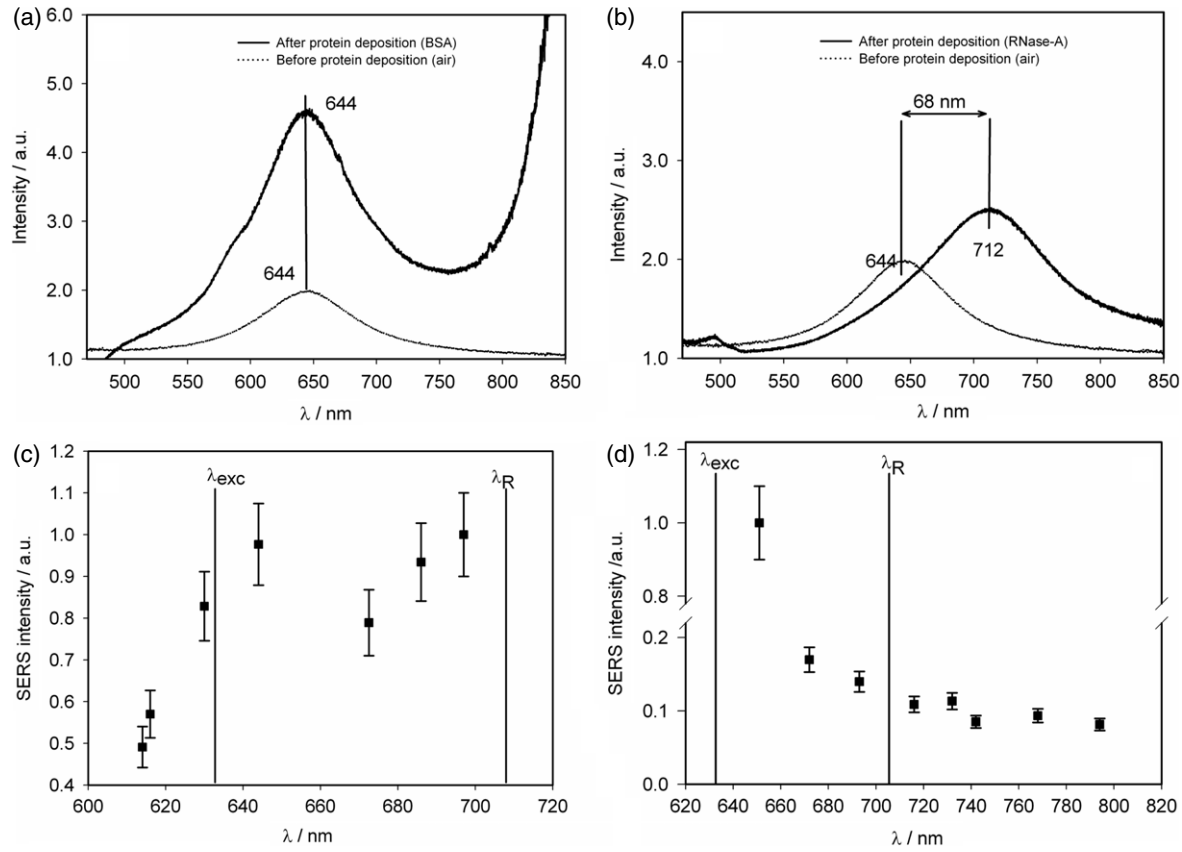

Figure 3. Extinction spectra measured for BSA (a) and RNase-A (b) in the case of nanocylinder arrays with a diameter of 140 nm, showing the shift of the position of the plasmon resonance due to the protein deposition on the nanoparticles with respect to the air. SERS intensity as a function of the position of the plasmon resonance calculated for the BSA Raman bands located at 1614 and 1658 cm^{-1} (c) and the RNase-A Raman bands located at 1614 cm^{-1} (d). The excitation wavelength (λ_{exc}) is 632.8 nm and the considered Raman band (λ_R) for BSA is located at 707 nm and for RNase-A at 705 nm. In order to make the error bars more readable in (d) we applied a break on the *Y* axis (between 0.22 and 0.78).

On the other hand, throughout this study we demonstrate that, by using the gold nanocylinder arrays obtained by the EBL method, it is possible to measure SERS spectra of BSA and RNase-A. In order to estimate the potential sensitivity of such a substrate, let us discuss the signal-to-noise ratio obtained with our Raman set-up. For BSA, this ratio is around 10 whereas it is around 60 for RNase-A. Thus, with such a ratio, we assume that lower concentrations of proteins can be detected with our SERS substrate. A limit of detection (LOD) can be estimated to be close to 10^{-4} M for BSA and between 10^{-4} and 10^{-5} M for RNase-A. These LOD are not very low but it is known that cylinders are not the most efficient nanoparticles to reach the highest enhancement factor. Thus, using other structures such as nanowires or coupled nanoparticles using EBL, we could decrease these LOD and increase the sensitivity of our SERS substrate. These reproducible SERS substrates can actually be used to develop a highly sensitive nanosensor chip for pathogen biosensor applications.

4. Conclusion

In this study, we have demonstrated that the lithographed gold nanocylinders obtained by the EBL technique provide SERS spectra of bovine serum albumin and ribonuclease-A at 1 mM concentration in aqueous solution. The reproducibility of the SERS substrate and thus of the SERS spectra of proteins can help us to better understand the origin of the SERS mechanism and to correlate its effects with the Raman intensity enhancement as shown in this paper. The gold nanocylinders are good candidates to reveal a significant SERS effect for proteins at 1 mM concentration, with a gain/molecule of about 10^5 for BSA and 10^7 for RNase-A. This SERS effect depends in a critical manner on the position of the Raman band maximum relative to the plasmon resonance wavelength. On the other hand, we have clearly proved that the Raman gain rises to a maximum when the LSP resonance wavelength is located between the laser excitation wavelength and that of the studied Raman mode.

Our results strongly suggest that these nanoparticles could be used to manufacture a highly reproducible SERS sensor. In order to determine the sensitivity of this SERS substrate, we have estimated the detection limit for these two proteins under the same experimental conditions (around 10^{-4} and 10^{-5} for BSA and RNase-A, respectively). Greater sensitivity and a high molecular specificity could be reached by a high degree of control and optimization of the sensor parameters: the nanoparticle geometrical parameters, their optical properties,

their enhancement factor and their functionalization. With such control, it is possible to reach a high level of reproducibility in the selectivity and the sensitivity of our sensor and in its main characteristics.

Acknowledgments

This work has been supported by FP7-HEALTH-F5-2009-241818-NANOANTENNA European project and the Conseil Régional de Champagne Ardenne.

References

[1] Kneipp K, Wang Y, Kneipp H, Perelman L T, Itzkan I, Dasari R R and Feld M S 1997 *Phys. Rev. Lett* **78** 1667–70
[2] Constatino C J L, Lemma T, Antunes P A and Aroca A 2001 *Anal. Chem.* **73** 3674
[3] Le Ru E C, Etchegoin P G and Meyer M 2006 *J. Chem. Phys.* **125** 204701
[4] Otto A 2006 *J. Raman Spectrosc.* **37** 937
[5] Blackie E J, Le Ru E C, Meyer M, Timmer M, Burkett B, Northcote P and Etchegoin P G 2008 *Phys. Chem. Chem. Phys.* **10** 4147–53
[6] Blackie E J, Le Ru E C and Etchegoin P G 2009 *J. Am. Chem. Soc.* **131** 14466–72
[7] Hu J, Sheng R S, Xu S Z and Zeng Y 1995 *Spectrochim. Acta* **51A** 1087–96
[8] Aroca R 2006 *Surface-Enhanced Vibrational Spectroscopy* (Chichester: John Wiley & Sons Ltd) pp 141–76
[9] Kneipp J 2006 Nanosensors based on SERS for applications in living cells *Surface-Enhanced Raman Scattering—Physics and Applications* ed K Kneipp, M Moskovits and H Kneipp (Heidelberg, Berlin: Springer)
[10] Lacharmoise P D, Le Ru E C and Etchegoin P G 2008 *ACS Nano* **3** 66–72
[11] Iosin M, Toderas F, Baldeck P L and Astilean S 2009 *J. Mol. Struct.* **924–926** 196–200
[12] Hudson S D and Chumanov G 2009 *Anal. Bioanal. Chem.* **394** 679–86
[13] Shafer-Peltier K E, Haynes C L, Glucksberg M R and Van Duyne R P 2003 *J. Am. Chem. Soc.* **125** 588–93
[14] Xu S, Ji X, Xu W, Zhao B, Duo X, Bai Y and Ozaki Y 2005 *J. Biomed. Opt.* **10** 031112
[15] Zhang X, Shah N C and Van Duyne R P 2006 *Vib. Spectrosc.* **42** 2006
[16] Douglas P, Stokes R J, Graham D and Smith W E 2008 *Analyst* **133** 791
[17] Qian X, Peng X H, Ansari D, Yin-Goen Q, Chen G Z, Shin D M, Yang L, Young A N, Wang M D and Nie S 2008 *Nat. Biotechnol.* **26** 83–90
[18] Stokes R J, McBride E, Wilson G C, Girkin J M, Smith W E and Graham D 2008 *Appl. Spectrosc.* **62** 371
[19] Das G, Mercarini F, Gentille F, De Angelis F, Kumar H G M, Candeloro P, Liberale C, Cuda G and Di Fabrizio E 2009 *Biosen. Bioelectron.* **24** 1693–9
[20] Haynes C L, McFarland A D and Van Duyne R P 2005 *Anal. Chem.* **77** 339A–46A
[21] Le Ru E C, Meyer M, Blackie E and Etchegoin P G 2008 *J. Raman Spectrosc.* **39** 1127–34
[22] Otto A 2001 *Phys. Status Solidi* **188** 1455–70
[23] Jeanmaire D L and Van Duyne R P 1977 *J. Electroanal. Chem.* **84** 1
[24] Félidj N, Aubard J and Levi G 2002 *Phys. Rev.* B **65** 075419
[25] Yonzon C R, Zhang X and Van Duyne R P 2003 *Proc. SPIE* **5224** 78–85
[26] Grand J, Lamy de la Chapelle M, Bijeon J L, Adam P-M, Vial A and Royer P 2005 *Phys. Rev.* B **72** 33407
[27] Billot L, Lamy de la Chapelle M, Grimault A-S, Vial A, Barchiesi D, Bijeon J-L, Adam P-M and Royer P 2006 *Chem. Phys. Lett.* **422** 303–7
[28] Guillot N, Shen H, Frémaux B, Peron O, Rinnert E, Toury T and Lamy de la Chapelle M 2010 *Appl. Phys. Lett.* **97** 1–3
[29] Félidj N, Aubard J and Levi G 2003 *Appl. Phys. Lett.* **82** 3095–97
[30] Liao P F 1982 *Surfaced-Enhanced Raman Scattering* ed K R Chang and T A Furtak (New York: Plenum) pp 315–79
[31] Bingler H G, Brunner H, Leitner A, Aussenegg F R and Wokaun F 1995 *Mol. Phys.* **85** 587
[32] Kahl M and Voges E 2000 *Phys. Rev.* B **61** 14078
[33] Weitz D A, Garoff S, Gersten J I and Nitzan A 1983 *J. Chem. Phys.* **79** 5324
[34] Goudonnet J P, Bijeon L J, Warmark R J and Ferrel T L 1991 *Phys. Rev.* B **43** 4605
[35] Creighton J A, Blatchford C G and Albrecht M G 1980 *J. Chem. Soc. Faraday Trans.* II **75** 790
[36] Keating C D, Kovalevski K M and Natan M J 1998 *J. Phys. Chem.* B **102** 9404–13
[37] Freeman R G *et al* 1995 *Science* **267** 1629
[38] Gotschy N W, Vonmetz K, Leitner A and Aussenegg F R 1996 *Opt. Lett.* **21** 1099
[39] Salerno M, Félidj N, Krenn J R, Leitner A and Aussenegg F R 2001 *Phys. Rev.* B **63** 165422
[40] Grand J, Koskcheev S, Bijeon J L, Lamy de la Chapelle M, Adam P M, Rumyantseva A, Lérondel G and Royer P 2003 *Synth. Met.* **139** 621–4
[41] Neubrech F, Kolb T, Lovrincic R, Fahsold G, Aizpurua J, Toimil-Molares M E, Karim S, Cornelius T W, Neumann R and Pucci A 2006 *Appl. Phys. Lett.* **89** 253104
[42] Grand J, Adam P-M, Grimault A-S, Vial A, Lamy de la Chapelle M, Bijeon J-L, Kostcheev S and Royer P 2006 *Plasmonics* **1** 135–40
[43] Li X L, Xu W Q, Zhang J H, Jia H Y, Yang B, Zhao B, Li B F and Ozaki Y 2004 *Langmuir* **20** 1298–304
[44] Nakamura K, Era S, Ozaki Y, Sogami M, Hayashi T and Murakami T 1997 *FEBS Lett.* **417** 375–8
[45] Sugio S, Kashima A, Mochizuki S, Noda M and Kobayashi K 1999 *Protein Eng.* **12** 439–46
[46] Chen M C and Lord R C 1976 *J. Am. Chem. Soc.* **98** 990–2
[47] Liang M, Chen V Y T, Chen H-L and Chen W 2006 *Talanta* **69** 1269–77
[48] Cavalu S, Cinta-Pinzaru S, Leopold N and Kiefer W 2001 *Biopolymers* **62** 341–8
[49] Yu N T, Jo B H and Liu C S 1972 *J. Am. Chem. Soc.* **94** 7572
[50] Koenig J L and Frushour B G 2004 *Biopolymers* **11** 2505–20
[51] Siamwiza M N, Lord R C, Chen M C, Takamatsu T, Harada I, Matsuura H and Shimanouchi T 1975 *Biochemistry* **14** 4870–6
[52] Van Dael H, Lafaut J P and Van Cauwelaert F 1987 *Eur. Biophysics J.* **14** (7) 409–14
[53] Jenkins A L, Larsen R A and Williams T B 2005 *Spectrochim. Acta* A **61** 1585–94